

基于数字脉冲整形技术的可变光谱宽度相位调制研究

龚雨枫^{1,2*}, 汪小超¹, 唐阳慧¹, 徐首英¹, 周申蕾^{1*}¹中国科学院上海光学精密机械研究所高功率激光物理联合实验室, 上海 201800;²中国科学院大学, 北京 100049

摘要 高功率激光驱动器中多采用谱色散匀滑(SSD)的束匀滑技术,而 SSD 中的相位调制常使用等幅相位调制。为进一步改善匀滑效果,提高动态调控能力,提出一种特异性相位调制技术,即采用调制深度为时变函数的特异性调制方式来获得光谱宽度可随时间变化的信号输出。基于相位调制的频谱理论,分析了特异性相位调制后的激光频谱特性。利用任意波形发生器(AWG)整形输出的特定相位调制信号开展实验研究,通过改变 AWG 输出两路电信号的相对时间差,得到 250 ps 的信号光在 3 ns 内不同时间点的调制光谱,实验结果与理论模拟结果一致。这种调制方式可以完成光谱宽度的连续实时调控,这对于高功率激光驱动器的激光参数控制中实现动态的光谱色散匀滑有着重要应用。

关键词 激光光学; 相位调制; 光谱宽度; 光谱色散匀滑; 惯性约束核聚变

中图分类号 O436

文献标志码 A

doi: 10.3788/CJL202148.2005003

1 引言

激光惯性约束核聚变(ICF)实现内爆的过程^[1],对靶面辐照的均匀性提出了一系列要求,并由此提出包括光谱色散匀滑(SSD)在内的多种光束匀滑技术^[2-8]。依据物理过程的不同,在不同时间段内采用不同的物理参数,能够进一步提高焦斑的平滑效果。以 OMEGA 装置为例,根据 SSD 功能^[9-10]其前端产生的主脉冲分为两部分,脉冲初始部分通过高频的多频相位调制实现大带宽输出以获得更好的平滑效果,主脉冲通过相对窄的光谱宽度输出实现平滑功能以及受激布里渊散射效应的抑制功能,最终通过合束形成一个完整的脉冲输出^[11-13]。显然,人们对 OMEGA 装置的主脉冲前端的脉冲光在不同时间点的调制要求不同,即光谱宽度需求不同,但其都是通过光束的时间与空间拼接来实现,光路系统相对复杂。本文提出一种利用特异性相位调制的可变光谱宽度方案,使用时变的调制深度函数,使不同时间点对应不同的调制度,从而引起相应的光谱宽度改变,实现无需分束调制即可满足脉冲光在

不同时间点具有不同光谱宽度的需求。同时,特异性相位调制可以提升光谱的实时调控能力,也可增加光束的调控维度。

2 特异性相位调制的设计原理及方法

2.1 一般等幅相位调制

电光效应可以通过改变外加电场来实现对晶体光学特性的影响。本文使用铌酸锂波导调制器进行相位调制^[14-17]。铌酸锂光波导常用的切割方式是 X 切 Y 传和 Z 切 Y 传,例如 Z 切 Y 传表示该铌酸锂波导调制器沿 Z 方向切割,光沿 Y 方向传播。它的电极位于光波导的下方,接入微波源。激光通过加载电压的铌酸锂波导相位调制器后,产生 $\Delta\varphi = \pi n_e^3 \gamma_{33} \Gamma \frac{V_0 L}{G \lambda} \cdot M(\omega)$ 的相位变化,其中: V_0 是沿 Z 轴加载的调制电场幅度; n_e 是非常光折射率; Γ 是重叠积分因子,表示光场与调制电场的相互作用强度,并且有 $0 < \Gamma < 1$; L 是电极的长度; G 是电极的间隙宽度; λ 是入射光的波长; γ_{33} 是铌酸锂晶体的电光系数; $M(\omega)$ 是描述调制电场的频率响应量。在高频

收稿日期: 2021-02-18; 修回日期: 2021-03-22; 录用日期: 2021-03-29

基金项目: 中科院先导项目(XDA25020304)

通信作者: *slzhou@mail.shenc.ac.cn; **gyf771876105@live.com

调制的情况下, 铌酸锂波导相位调制器的半波电压可以表示为

$$V_{\pi} = \frac{\lambda G}{n_e^3 \gamma_{33} \Gamma \cdot M(\omega)} \quad (1)$$

在加载高频调制信号进行相位调制时, 加载至波导上的高频调制信号幅度会受到相位匹配和微波损耗的影响, 所以需通过 $M(\omega)$ 来描述频率对调制的影响。

经过电光相位调制器的调制后, 激光的电场可以表示为

$$E = A_0 \cdot \exp\{i[\omega_0 t + \sigma_M \sin(\omega_M t)]\}, \quad (2)$$

式中: ω_M 是调制角频率; σ_M 是相位调制的调制深度, 一般情况下可视作常数。显然相位调制函数为 $f(t) = \sigma_M \sin(\omega_M t)$ 。此时的电场可以利用雅可比-安格尔恒等式表示为

$$E_M(\mathbf{r}_T, t) = E_0(\mathbf{r}_T, t) \cdot \exp[i\sigma_M \sin(\omega_M t)] = E_0(\mathbf{r}_T, t) \cdot \sum_{m=-\infty}^{\infty} J_m(\sigma_M) \exp(im\omega_M t), \quad (3)$$

式中: $J_m(\cdot)$ 是第 m 阶的贝塞尔函数, 而 m 是整数; \mathbf{r}_T 为空间位移矢量。(3)式对应的复合角谱则可以表示为

$$\tilde{E}_M(\mathbf{k}_T, \omega) = \tilde{E}_0(\mathbf{k}_T, \omega) \otimes \sum_{m=-\infty}^{\infty} J_m(\sigma_M) \delta(\omega - m\omega_M), \quad (4)$$

式中 $\delta(\cdot)$ 为狄拉克函数; \otimes 表示卷积; \mathbf{k}_T 为空间波矢量。(4)式表示经过相位调制后的脉冲激光角谱变为一系列频率间隔为 ω_M 的角谱, 它的形状与初始角谱 $\tilde{E}_0(\mathbf{k}_T, \omega)$ 相同, 大小幅度由 $J_m(\sigma_m)$ 决定^[18]。

2.2 特异性相位调制

一般情况下的相位调制的调制深度 σ_M 都是一个常数, 但是在特异性调制下调制深度是一个时变函数即 $\sigma_M(t)$ 。此时, 特异性相位调制的调制函数可以表示为

$$f(t) = \sigma_M(t) \sin(\omega_M t). \quad (5)$$

特异性相位调制的目的是根据主脉冲前端的脉冲光在不同时间点的调制要求不同, 设计调制深度函数 $\sigma_M(t)$ 。首先根据实验所需的相位变化, 预设一个相位变化的目标函数 $\varphi'(t)$, 对 $\varphi'(t)$ 进行积分得到其基本调制函数形式 $f(t)$, 即(5)式。此时激光的电场可以利用雅可比-安格尔恒等式表示为

$$E_M(\mathbf{r}_T, t) = E_0(\mathbf{r}_T, t) \cdot \exp[i\sigma_M(t) \sin(\omega_M t)] = E_0(\mathbf{r}_T, t) \cdot \sum_{m=-\infty}^{\infty} J_m[\sigma_M(t)] \exp(im\omega_M t), \quad (6)$$

其对应的复合角谱则可以表示为

$$\tilde{E}_M(\mathbf{k}_T, \omega) = \tilde{E}_0(\mathbf{k}_T, \omega) \otimes \sum_{m=-\infty}^{\infty} \mathcal{F}\{J_m[\sigma_M(t)]\} \delta(\omega - m\omega_M), \quad (7)$$

式中 $\mathcal{F}\{\cdot\}$ 表示傅里叶变换。(7)式表示经过相位调制后的脉冲激光角谱变为一系列频率间隔为 ω_M 的角谱, 它的形状与初始角谱 $\tilde{E}_0(\mathbf{k}_T, \omega)$ 相同, 大小幅度由 $\sum_{m=-\infty}^{\infty} \mathcal{F}\{J_m[\sigma_M(t)]\}$ 决定, 但是该项的形式相对复杂, 需要结合具体 $\sigma_M(t)$ 函数来分析。

3 实验验证与分析

3.1 具体特异性相位调制函数的设计及分析

为获得一个光谱宽度逐渐增大的调制输出, 目标相位变化函数是一个随时间震荡的函数形式, 且振幅递增, 即 $\varphi'_1(t) = kt \cdot \sin(\omega_M t)$, 如图 1 所示。

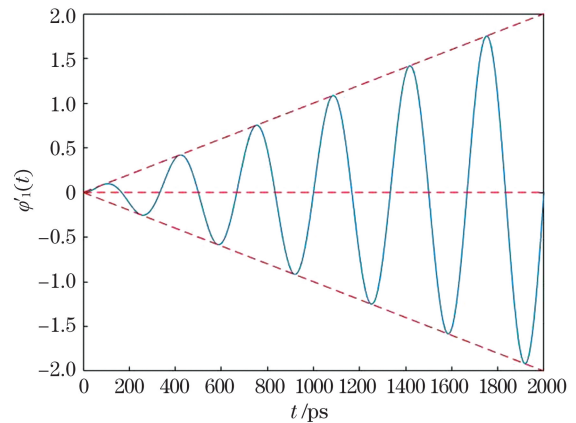


图 1 $\varphi'_1(t)$ 随时间变化示意图

Fig. 1 Schematic diagram of $\varphi'_1(t)$ changing with time

根据图 1 可得

$$f_1(t) = \int \varphi'_1(t) dt = \frac{k}{\omega_M^2} \sin(\omega_M t) - \frac{kt}{\omega_M} \cos(\omega_M t), \quad (8)$$

式中 k 为线性调制系数。(8)式中的调制深度函数则可以表示为 $\sigma_1(t) = \frac{f_1(t)}{\sin(\omega_M t)} = \frac{k}{\omega_M^2} - \frac{kt \cos(\omega_M t)}{\omega_M \sin(\omega_M t)}$ 。利用雅可比-安格尔恒等式, 根据(6)式的推导可得相位调制函数调制后的激光电场为

$$\tilde{E}_M(t) = \sum_{n=-\infty}^{\infty} J_n\left(\frac{k}{\omega_M^2}\right) \exp(in\omega_M t) \cdot \sum_{m=-\infty}^{\infty} (-i)^m J_m\left(\frac{kt}{\omega_M}\right) \exp(im\omega_M t), \quad (9)$$

根据(7)式, 对(9)式进行傅里叶变换后, 可得

$$\begin{aligned} \tilde{E}_M(\omega) = & \sum_{n=-\infty}^{\infty} J_n\left(\frac{k}{\omega_M}\right) \delta(\omega - m\omega_M) \otimes \\ & \left[\sum_{m=-\infty}^{\infty} (-i)^m \mathcal{F}\left\{J_m\left(\frac{kt}{\omega_M}\right)\right\} \otimes \delta(\omega - m\omega_M) \right]. \end{aligned} \quad (10)$$

(10)式根据贝塞尔函数的特点可得

$$\begin{aligned} \mathcal{F}\left\{J_m\left(\frac{kt}{\omega_M}\right)\right\} = & \\ \frac{\left|\frac{\omega_M}{k}\right| \sqrt{\frac{2}{\pi}} (-i)^m T_m\left(\frac{\omega_M}{k} \cdot \omega\right) \text{rect}\left(\frac{\omega_M}{k} \cdot \omega\right)}{\sqrt{1 - \left(\frac{\omega_M}{k} \cdot \omega\right)^2}}, \end{aligned} \quad (11)$$

式中: $T_m(\cdot)$ 为 m 次的切比雪夫多项式, $\text{rect}(\cdot)$ 为矩形函数。此时将 (11) 式代入 (10) 式中, 就可以得到最终的傅里叶变换后的频谱函数。

同样对于一个光谱宽度逐渐减小的调制输出, 目标函数同样是一个随时间震荡的函数形式, 但是振幅递减, 即 $\varphi'_2(t) = (t_0 - kt) \cdot \sin(\omega_M t)$, 如图 2 所示。

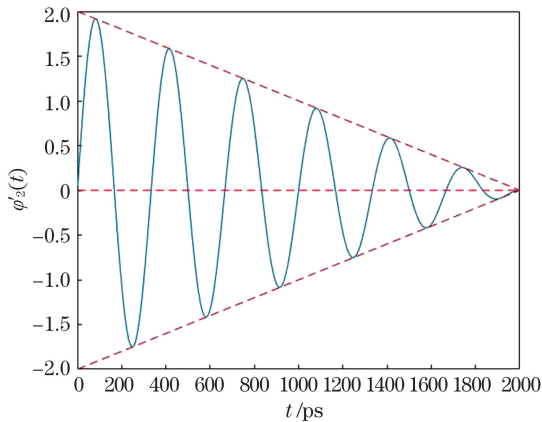


图 2 $\varphi'_2(t)$ 随时间变化示意图

Fig. 2 Schematic diagram of $\varphi'_2(t)$ changing with time

此时对 $\varphi'_2(t)$ 的处理方法与对 $\varphi'_1(t)$ 的处理方法相同, 即

$$\begin{aligned} f_2(t) = & \int \varphi'_2(t) dt = \\ & \frac{t_0 - kt}{\omega_M} \cos(\omega_M t) - \frac{k}{\omega_M^2} \sin(\omega_M t), \end{aligned} \quad (12)$$

其频谱为

$$\begin{aligned} \tilde{E}_M(\omega) = & \sum_{n=-\infty}^{\infty} (-1)^n J_n\left(\frac{k}{\omega_M}\right) \delta(\omega - m\omega_M) \otimes \\ & \left[\sum_{m=-\infty}^{\infty} i^m \mathcal{F}\left\{J_m\left(\frac{kt}{\omega_M}\right)\right\} \otimes \delta(\omega - m\omega_M) \right]. \end{aligned} \quad (13)$$

(13)式根据贝塞尔函数的特点可得

$$\begin{aligned} \mathcal{F}\left\{J_m\left(\frac{t_0 - kt}{\omega_M}\right)\right\} = & \mathcal{F}\left\{J_m\left(\frac{kt}{\omega_M}\right)\right\} \exp(it_0\omega) = \\ & (-1)^m \frac{\left|\frac{\omega_M}{k}\right| \sqrt{\frac{2}{\pi}} (-i)^m T_m\left(\frac{\omega_M}{k} \cdot \omega\right) \text{rect}\left(\frac{\omega_M}{k} \cdot \omega\right)}{\sqrt{1 - \left(\frac{\omega_M}{k} \cdot \omega\right)^2}} \cdot \\ & \exp(it_0\omega). \end{aligned} \quad (14)$$

此时将 (14) 式代入 (13) 式中可得到最终的傅里叶变换后的频谱函数。

3.2 特异性相位调制的实验

基于特异性相位调制的高频特性, 需要在纳秒级的激光脉冲时间尺度内进行实验, 得到与相位调制函数相对应的电压值, 并将其加载至相位调制器上, 对单纵模光纤激光器发出的脉冲激光进行调制。由于不同时间点处的调制度不同, 而脉冲激光的脉宽是有限的, 故只能测量一段调制时间内的脉冲光光谱。

经过特异性相位调制的光谱变化的测量装置如图 3 所示: 先利用任意波形发生器(AWG)的通道 1 产生一个脉冲电信号 $E_p(t)$, 该信号经电放大器放大后加载至偏置调制器上, 该过程将连续的激光调制成脉冲光进行输出; 设计的具有特异性相位调制函数 $f(t)$ 的信号通过任意波形发生器的通道 2 进行数字脉冲整形, 再经过电放大器放大后加载至相位调制器上。

实验中使用的任意波形发生器是 Tektronix 的 AWG7122C, 它的采样率为 12 GSa/s, 采样间隔为 83 ps。相位调制器使用的是 Thorlabs 的铌酸锂电光调制器, 输入和输出都是使用光纤耦合, 半波电压为 $U_\pi = 3.9$ V。通道 1 产生的脉冲信号光, 其脉宽为 250 ps, 中心波长为 1053 nm, 用于测量相位调制在不同时间段内对激光光谱宽度的改变。如图 4 所示, 实验中通过改变 AWG 的两个通道的输出时间延迟来改变不同调制时间段下的脉冲特性, 最后利用“体光栅+面 CCD”的自研光谱仪测量输出脉冲光的光谱宽度, 光谱仪的测试精度为 0.873 pm。

实验在 3 ns 时间内一共测试了 37 组调制脉冲光光谱数据。以 $f_1(t)$ 调制为例, 在每个延迟时间点下都获取一组 CCD 图像, 图 5 给出 6 个延迟时间点的调制时段内对应的光谱宽度: 当 $t = 1$ ps 时, 光谱宽度为 $\Delta\lambda = 0.0121$ nm; 当 $t = 664$ ps 时, 光谱宽度为 $\Delta\lambda = 0.0288$ nm; 当 $t = 1245$ ps 时, 光谱宽度为 $\Delta\lambda = 0.0707$ nm; 当 $t = 1826$ ps 时, 光谱宽度为 $\Delta\lambda = 0.0934$ nm; 当 $t = 2407$ ps 时, 光谱宽度为 $\Delta\lambda = 0.1152$ nm; 当 $t = 2988$ ps 时, 光谱宽度为 $\Delta\lambda = 0.0218$ nm。

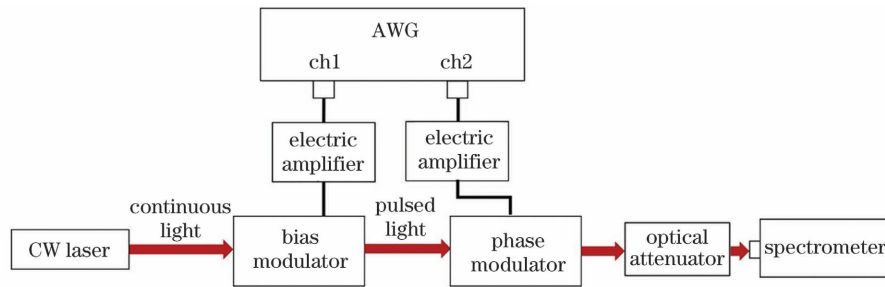


图 3 特异性相位调制的光谱变化实验装置示意图

Fig. 3 Schematic diagram of spectral change experimental device for specific phase modulation

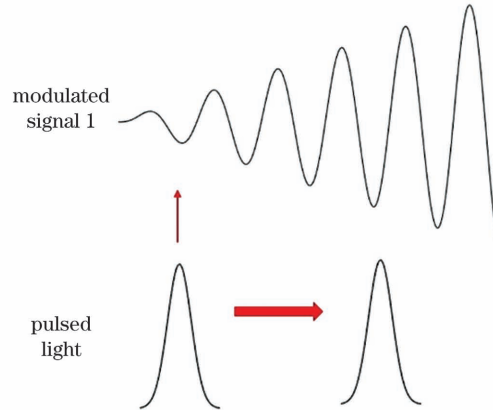


图 4 改变脉冲光与调制信号的相对位置实现光谱展宽示意图

Fig. 4 Schematic diagram of spectral broadening obtained by changing the relative position of pulsed light and modulated signal

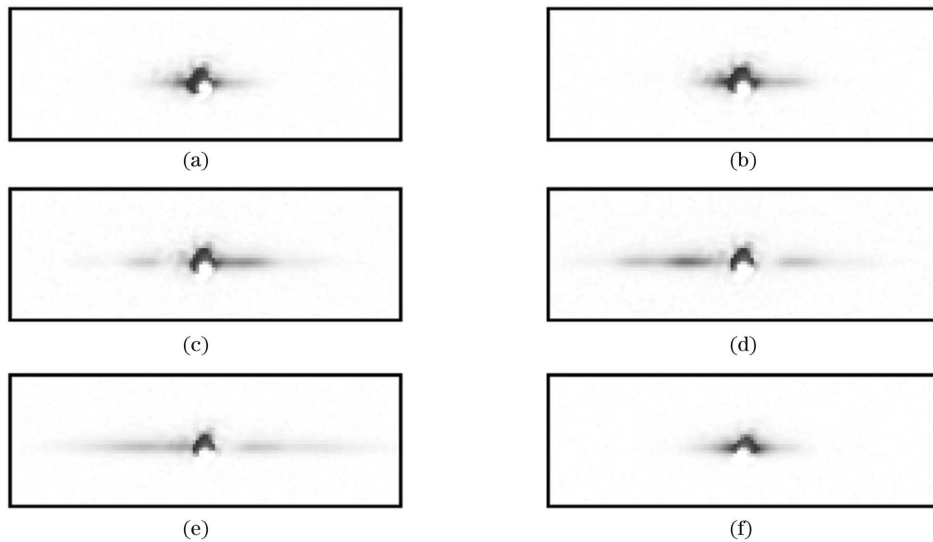


图 5 $f_1(t)$ 调制不同时间段时 CCD 获得的光谱图。(a) $t=1$ ps; (b) $t=664$ ps; (c) $t=1245$ ps; (d) $t=1826$ ps; (e) $t=2407$ ps; (f) $t=2988$ ps

Fig. 5 Spectrum images obtained by CCD for $f_1(t)$ -modulating at different time. (a) $t=1$ ps; (b) $t=664$ ps; (c) $t=1245$ ps; (d) $t=1826$ ps; (e) $t=2407$ ps; (f) $t=2988$ ps

3.3 实验结果的分析

实验中, 3 ns 的时间范围内, 每次移动 37 个采样点, 此时脉冲信号光的脉宽为 $\Delta t=250$ ps。根据 (8) 式的调制函数 $f_1(t)$ 与 (12) 式的调制函数 $f_2(t)$ 所对应的调制度, 可得

$$\Delta\omega_i = \left| \omega_{\text{Max}} - \omega_{\text{Min}} \right|_{t_i - \frac{\Delta t}{2}}^{t_i + \frac{\Delta t}{2}} = \left| \varphi'_{\text{Max}} - \varphi'_{\text{Min}} \right|_{t_i - \frac{\Delta t}{2}}^{t_i + \frac{\Delta t}{2}}, \quad (15)$$

将 (15) 式代入到 $\Delta\lambda = \frac{\lambda}{c} \cdot \frac{\Delta\omega}{2\pi}$ 中, 再加上原始信号

光未调制时的光谱宽度,就可以模拟得到经过调制后的脉冲信号光的光谱宽度。

图 6 给出调制函数 $f_1(t)$ 下的输出脉冲光光谱宽度图,实线表示经过 $f_1(t)$ 不同时间段调制的脉冲信号光光谱宽度变化,虚线表示 $f_1(t)$ 调制下不同时间调制的脉冲信号光光谱宽度变化的模拟结果。在 $f_1(t)$ 的调制下,脉冲光的光谱宽度先缓慢增大,后随着调制度的迅速增大而显著增大,且呈锯齿状震荡;受光谱仪测量精度的影响,实验结果的震荡幅度相对较大。由于信号光具有一定的时间宽度,实验中光谱的展宽在初始和末尾分别出现延迟与拖尾现象。若采样间隔不变,减小信号光脉宽,谱宽的震荡幅度会随时间的增加而加大;若信号光脉宽不变,减小采样间隔,这种锯齿状震荡会更加平滑;减小信号光脉宽的同时减小采样间隔,信号光光谱宽度的震荡幅度递增,并且更加接近相位变化函数的绝对值 $|\varphi'_1(t)|$ 。

图 7 给出调制函数 $f_2(t)$ 下的输出脉冲光光谱宽度图,实线表示经过 $f_2(t)$ 不同时间段调制的脉

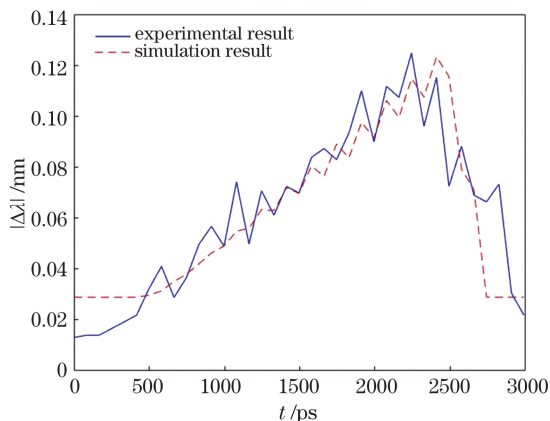


图 6 调制函数 $f_1(t)$ 下的输出脉冲光光谱宽度

Fig. 6 Spectrum width of $f_1(t)$ -modulated pulsed light

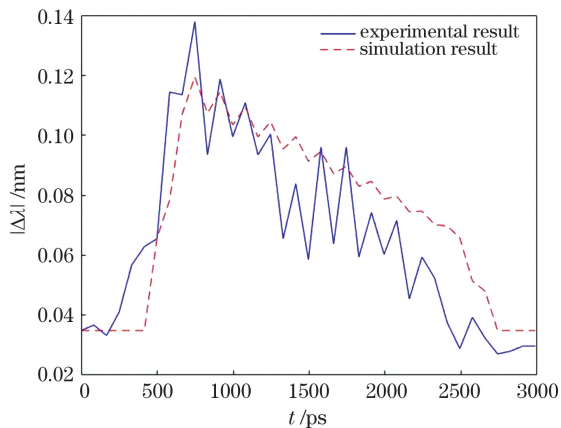


图 7 调制函数 $f_2(t)$ 下的输出脉冲光光谱宽度图

Fig. 7 Spectrum width of $f_2(t)$ -modulated pulsed light

冲信号光的光谱宽度变化,虚线表示在 $f_2(t)$ 调制下不同时间段调制的脉冲信号光光谱宽度变化的模拟结果。在 $f_2(t)$ 调制下,信号光光谱宽度先迅速增大,达到最大值后呈锯齿状震荡减小,实验结果与模拟结果一致。而在 2400~2800 ps 调制函数的尾部,由于该段的调制度较小,信号光脉宽时间内的调制度变化更弱,分析和实验均表明尾部时间段内光谱宽度迅速减小。

4 结 论

提出一种特异性相位调制函数的方法,设计出时变相位调制函数并分析其物理过程,该函数作用下的相位调制可以有效实现信号光光谱宽度随时间的变化。实验结果表明,在本研究提出的相位调制函数的作用下,信号光的光谱宽度均随时间增加出现震荡,且震荡振幅递增或递减,这与模拟分析结果一致,验证了实时动态调控光谱的可行性。在实际应用中,可以使用更大功率的电放大器来获取更高的调制电压输出,以实现更宽的光谱宽度调节。特异性相位调制研究可为改善时域平滑性能、实现光谱宽度的动态控制进而提升高功率激光的调控能力提供理论参考。

参 考 文 献

- [1] Zhu J Q, Zhu J, Li X C, et al. Status and development of high-power laser facilities at the NLHPLP[J]. High Power Laser Science and Engineering, 2018, 6: e55.
- [2] Marozas J A, Kelly J H, Angular spectrum representation of pulsed laser beams with two dimensional smoothing by spectral dispersion [J]. Laboratory for Laser Energetics Review, 1999, 78: 62-81.
- [3] Rothenberg J E. Comparison of beam-smoothing methods for direct-drive inertial confinement fusion [J]. Journal of the Optical Society of America B, 1997, 14(7): 1664-1972.
- [4] Lehmborg R H, Rothenberg J E. Comparison of optical beam smoothing techniques for inertial confinement fusion and improvement of smoothing by the use of zero-correlation masks [J]. Journal of Applied Physics, 2000, 87(3): 1012-1022.
- [5] Hocquet S, Lacroix G, Penninckx D. Compensation of frequency modulation to amplitude modulation conversion in frequency conversion systems [J]. Applied Optics, 2009, 48(13): 2515-2521.
- [6] Rothenberg J E. Improved beam smoothing with SSD using generalized phase modulation [J]. Proceedings

- of SPIE, 1997, 3047: 713-724.
- [7] Rothenberg J E. Two-dimensional beam smoothing by spectral dispersion for direct-drive inertial confinement fusion[J]. Proceedings of SPIE, 1995, 2633: 634-644.
- [8] Sun Z M, Liu D A, Han L, et al. Study on gain bandwidth characteristics of DKDP-OPCPA based on electro-optic modulation [J]. Chinese Journal of Lasers, 2020, 47(10): 1008001.
孙子茗, 刘德安, 韩璐, 等. 基于电光调制的 DKDP 晶体 OPCPA 增益带宽特性研究 [J]. 中国激光, 2020, 47(10): 1008001.
- [9] Zhang R, Jia H T, Tian X C, et al. Research of beam conditioning technologies using continuous phase plate, multi-FM smoothing by spectral dispersion and polarization smoothing[J]. Optics and Lasers in Engineering, 2016, 85: 38-47.
- [10] Zhang R. Research on precise control technologies of intensity distribution on target of high power laser facilities [D]. Hefei: University of Science and Technology of China, 2013: 34-45.
张锐. 高功率激光装置靶面光强分布精密控制技术研究[D]. 合肥: 中国科学技术大学, 2013: 34-45.
- [11] Hohenberger M, Shvydky A, Marozas J A, et al. Optical smoothing of laser imprinting in planar-target experiments on OMEGA EP using multi-FM 1-D smoothing by spectral dispersion [J]. Physics of Plasmas, 2016, 23(9): 092702.
- [12] Liu X, Chen H M, Hu Y C. An integrated device for photonic-crystal electro-optic modulation and coarse wavelength-division multiplexing[J]. Chinese Journal of Lasers, 2021, 48(3): 0306002.
刘雪, 陈鹤鸣, 胡宇宸. 光子晶体电光调制和粗波分复用集成器件研究 [J]. 中国激光, 2021, 48(3): 0306002.
- [13] Zhou P W, Lu T, Lü J Y. Dither-adaptive laser pulse modulation technique for electro-optic modulator[J]. Chinese Journal of Lasers, 2020, 47(6): 0601001.
周鹏威, 卢田, 吕晋阳. 导频自适应的电光调制器激光脉冲调制技术 [J]. 中国激光, 2020, 47(6): 0601001.
- [14] Guo F Z, Yu C T, Tetsuro K. Quasi velocity matched electrooptic phase modulator [J]. Chinese Journal of Lasers, 1997, 24(4): 307-309.
郭凤珍, 于长泰, 小林哲郎. 准速度匹配电光相位调制器 [J]. 中国激光, 1997, 24(4): 307-309.
- [15] Pu H T, Li W, Xue Q, et al. Study of spectral widening characteristics of a waveguide phase modulator [J]. Chinese Journal of Lasers, 1998, 25(3): 261-264.
濮宏图, 李伟, 薛泉, 等. 波导相位调制器光谱展宽特性分析及实验研究 [J]. 中国激光, 1998, 25(3): 261-264.
- [16] Li Y, Zhang X X, Liu Y X. Optimal design of optical waveguide modulator[J]. Infrared, 2007, 28(4): 5-8.
李瑛, 张晓霞, 刘玉喜. 波导调制器的优化设计 [J]. 红外, 2007, 28(4): 5-8.
- [17] Cui H J. Research on broadband LiNbO₃ electrooptical modulators with integrated optical waveguides[D]. Chengdu: University of Electronic Science and Technology of China, 2003: 5-11.
崔海娟. 集成光波导宽带 LiNbO₃ 电光调制器研究 [D]. 成都: 电子科技大学, 2003: 5-11.
- [18] Jiang Y E. Research of beam smoothing technologies used under high-fluence conditions [C]. Beijing: Shanghai Institute of Optics and Mechanics, Chinese Academy of Sciences, 2013: 40-62.
姜有恩. 高通量条件下的光束匀滑技术研究 [D]. 北京: 中国科学院上海光学精密机械研究所, 2013: 40-62.

Phase Modulation Research on Variable Spectral Width Based on Digital Pulse Shaping Technology

Gong Yufeng^{1,2*}, Wang Xiaochao¹, Tang Yanghui¹, Xu Shouying¹, Zhou Shenlei^{1*}

¹ National Laboratory on High Power Laser and Physics, Shanghai Institute of Optics and Fine Mechanics, Chinese Academy of Sciences, Shanghai 201800, China;

² University of Chinese Academy of Sciences, Beijing 100049, China

Abstract

Objective In the implosion process of laser inertial confinement fusion (ICF), several requirements are proposed for the uniformity of the target irradiation and various beam-smoothing techniques, including spectral dispersion smoothing (SSD), have been developed and applied. According to different physical processes, different physical parameters are adopted in different periods to further improve the focal spot smoothing effect. Considering OMEGA

as an example, the main pulse generated by its front end is divided into two parts, corresponding to SSD. In the initial part of the pulse, high-frequency multifrequency phase modulation is used to achieve a wide bandwidth output to obtain a better smoothing effect. The relatively narrow spectral width output can smooth the main pulse and suppress the stimulated Brillouin scattering. Finally, the initial part of the pulse and the main pulse form a complete pulse output through the beam combination. The modulation requirements of the pulse light in the main pulse front end of the OMEGA device differ at different time points. However, the pulse light in the main pulse front end of the OMEGA device is realized by splicing time and space; the optical system is relatively complex. Therefore, it is necessary to implement a scheme that can achieve different modulations at different time points, changing the corresponding spectral width. The scheme can meet different spectral width requirements of different time points in the pulse light without beam-splitting modulation.

Methods This study investigates the specific phase modulation technology. The specific phase modulation function is obtained by integrating original phase change function of the target. It is essential that the modulation depth of the specific phase modulation function is a time-varying function. The spectrum width can be changed at any time using a specific phase modulation function to modulate the phase of the pulse light. Based on phase modulation spectrum theory, the spectrum characteristics of the laser with a specific phase modulation are analyzed. Using an arbitrary waveform generator (AWG) for digital pulse shaping, two output channels of AWG are used to output specific phase-modulated electrical signal and pulse shaping signal, respectively. After amplifying the two signals of two output channels of AWG using two electric amplifiers, the pulse shaping signal is connected to the bias modulator to shape the output of the continuous wave (CW) laser into the pulse optical input phase modulator. Additionally, a specific phase-modulated electrical signal is loaded onto the phase modulator. The modulation spectrum of 250-ps signal light at different time points in 3 ns is obtained by changing the relative time difference of two electrical signal outputs using AWG. The experimental results are consistent with the theoretical simulation.

Results and Discussions To obtain a modulation output with gradually increasing spectral width, phase modulation function $f_1(t)$ is obtained by integrating the target phase change function $\varphi'_1(t)$ (Fig. 1). Under the modulation of $f_1(t)$, the spectrum (Fig. 6) of the pulse light increases slowly at first. Then, the spectrum width significantly increases as the modulation depth increases, vibrating in a zigzag pattern. The oscillation amplitude of the experimental results is relatively large due to the influence of the measurement accuracy of the spectrometer. Since the signal light has a certain time width, the broadening of the spectrum appears delay and tailing at the beginning and end of the experiment, respectively. If the sampling interval is constant and the signal pulse width is reduced, the oscillation amplitude of the spectrum width with time will increase. However, if the pulse width of the signal light remains unchanged and the sampling interval is reduced, the zigzag oscillation will be smoother. If the pulse width of the signal light is reduced and the sampling interval is reduced, the spectrum width of the signal light changes with increasing oscillation, and it is closer to the absolute value of the phase change function $|\varphi'_1(t)|$. To obtain a modulation output with gradually decreasing spectral width, the phase modulation function $f_2(t)$ is obtained by integrating the target phase change function $\varphi'_2(t)$ (Fig. 2). Under the modulation of $f_2(t)$, the spectral width (Fig. 7) of the signal light increases rapidly at first, reaches the maximum value, and then decreases in zigzag oscillation. The experimental results are consistent with the results of the simulation. At the tail of the $f_2(t)$ modulation function, the modulation is smaller, and the modulation change is weaker in the pulse width of the signal light. The analysis and experiment show that the spectrum width decreases rapidly in tail time.

Conclusions This study proposes a method of specific phase modulation function. The corresponding time-varying phase modulation function is designed, and its physical process is analyzed. The phase modulation under the function can effectively realize the change in signal light spectral width with time. The experimental results show that under the effect of the designed phase modulation function, the spectral width of the signal light increases or decreases with time. It is consistent with the results of the simulation and verifies the feasibility of the real-time dynamic control of the spectrum. In practical applications, a higher power amplifier can achieve higher modulation voltage output and wider spectrum width adjustment. The research of the specific phase modulation can provide theoretical reference to improve the time domain-smoothing performance, realize dynamic control of spectral width, and improve the control ability of high-power lasers.

Key words laser optics; phase modulation; spectrum width; smoothing by spectral dispersion; inertial confinement fusion

OCIS codes 120.5060; 140.3300; 070.4790